A Random Sampling-Rate MPPT Method to Mitigate Interharmonics from Cascaded H-Bridge Photovoltaic Inverters

Pan, Yiwei; Sangwongwanich, Ariya; Yang, Yongheng; Blaabjerg, Frede

Published in:
Proceeding of 2020 IEEE 9th International Power Electronics and Motion Control Conference (IPEMC2020-ECCE Asia)

DOI (link to publication from Publisher):
10.1109/IPEMC-ECCEAsia48364.2020.9367929

Publication date:
2020

Document Version
Accepted author manuscript, peer reviewed version

A Random Sampling-Rate MPPT Method to Mitigate Interharmonics from Cascaded H-Bridge Photovoltaic Inverters

Yiwei Pan, Ariya Sangwongwanich, Yongheng Yang, and Frede Blaabjerg
Department of Energy Technology, Aalborg University
Pontoppidanstraede 111, Aalborg 9220, Denmark
E-mails: {ypa, ars, yoy, fbl}@et.aau.dk

***Abstract*—Interharmonics have become one challenging issue in power systems. One potential source of interharmonic emissions from photovoltaic (PV) systems is the perturbation of the maximum power point tracking (MPPT). In cascaded H-bridge (CHB) PV inverters, if the MPPT perturbations of CHB cells are in-phase, the oscillation on the equivalent total DC voltage will be multiplied, leading to large interharmonics in the grid. To address this issue, a phase-shifting MPPT (PS-MPPT) can be adopted. However, the interharmonic suppression performance of the PS-MPPT method is limited for CHB PV inverters with an odd number of cells. Moreover, when some CHB cells are operating under varying environmental conditions, the PS-MPPT may fail to minimize the oscillation on the total DC voltage, and thus, interharmonics appear again. To overcome these limitations, a random sampling-rate MPPT method for the CHB PV inverter is proposed in this paper. By randomly selecting the MPPT sampling-rate of each CHB cell, the dominant interharmonics can be effectively suppressed. Compared with the original PS-MPPT, the proposed method performs better in dynamic conditions in terms of interharmonic suppression, especially for CHB PV inverters with an odd number of cells. Simulations and experimental results have validated the effectiveness of the proposed method.**

***Keywords*—Cascaded H-bridge (CHB), interharmonics, maximum power point tracking (MPPT), photovoltaic (PV) systems, power quality.**

I. INTRODUCTION

Interharmonics are gaining significant attentions with the growing installation of PV systems, due to their potential to induce voltage fluctuation, sub-synchronous oscillations, light flickering and unintentional tripping of protection circuits [1]-[3]. Therefore, as recommended by the IEEE Standard 1547-2018, the interharmonic current distortion should be limited in a certain range for distributed energy resources [4]. For PV inverters, it has been revealed in the literature that the MPPT perturbation is one potential source of interharmonic emissions [2], [3]. This is because the low frequency oscillation caused by the MPPT will be reflected on the amplitude of the grid currents, and through the convolution with the grid phase-angle, interharmonics will emerge in the grid current [5], [6].

To address the interharmonic issue caused by the MPPT from PV inverters, the analysis, modeling, and mitigation of interharmonics from PV inverters have been discussed in the literature [6]-[8]. One simple way to mitigate interharmonics is to reduce the MPPT sampling rate [7]. However, this method will inevitably slow down the MPPT dynamics, and thus affect the MPPT efficiency. In [8], the interharmonics were suppressed by limiting the abrupt change of the current reference, whereas the suppression performance is not significant, since the periodical perturbation of the MPPT still exists. A random sampling-rate MPPT method has been presented in [7], where the sampling-rate of the MPPT was random for the next MPPT cycle. By doing so, the interharmonic contents can be distributed in a wider frequency range, and the amplitude of the dominant interharmonics can be effectively suppressed. Nevertheless, prior-art interharmonic mitigation methods are mainly for single-phase two-level inverters.

In a large-scale PV system, the CHB configuration has been introduced due to its modularity, high efficiency, and improved harmonic performance [9]-[11]. The overall diagram of the CHB PV inverter is shown in Fig. 1, where the PV panels are directly interfaced to the DC side of CHB cells. Clearly, if the MPPT perturbations are in-phase, the oscillation on the equivalent total DC voltage (sum of the voltages of all CHB cells) will be amplified, as shown in Fig. 2, where the voltage references of a 4-cell CHB PV inverter are exemplified, leading to larger interharmonics in the grid current [12]. To address the interharmonic issue in the cascaded converters, in [13], a DC voltage feed-forward control has been introduced. However, this method is not capable to reduce the interharmonics caused by the MPPT. More recently, a phase-shifting MPPT (PS-MPPT) method has been illustrated in [12] for CHB PV inverters, where the phase-angle of the DC voltage oscillation for each cell was detected and adjusted in a way to counteract with each other. By doing so, the oscillation in the equivalent total DC voltage can be mitigated, and thereby, the interharmonics. Nevertheless, when an odd number of converters are cascaded, no matter how to do the phase-shift, a small oscillation will still emerge in the equivalent total DC voltage. It means that the PS-MPPT has limited capability to suppress the dominant interharmonics [12]. Moreover, when part of the CHB cells are operating under dynamic conditions, e.g., varying environments (irradiance and temperature), the DC voltage oscillation of all cells will not be optimally phase-shifted. Subsequently, the interharmonic suppression performance will be degraded. Therefore, the PS-MPPT method cannot effectively suppress interharmonics under varying environmental conditions, especially with a high number of CHB cells.

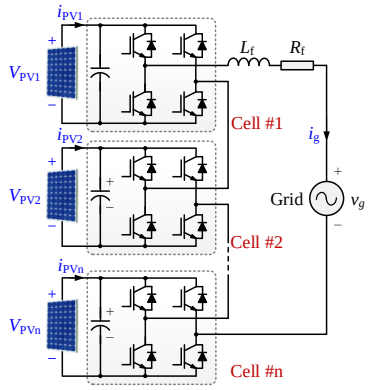

Fig. 1. Topology of a single-phase CHB PV inverter, where i_{PVk} and V_{PVk} (k = 1, 2, ..., n) represent the corresponding current and voltage of the k^{th} cell, L_f and R_f are the output AC filter impedance, and v_g and i_g are the grid voltage and current, respectively.

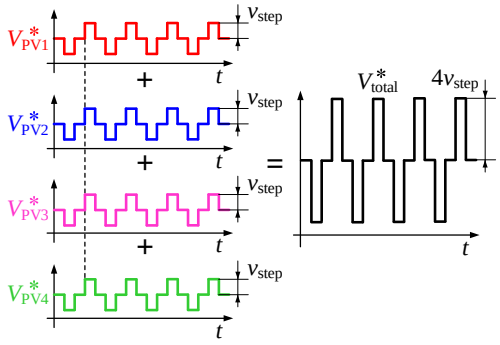

Fig. 2. Illustration of the in-phase oscillation phenomenon on a 4-cell CHB PV inverter, where V^*_{PVk} is the voltage reference for the k^{th} cell, v_{step} is the MPPT perturbation step size, and V^*_{total} is the equivalent total DC voltage reference.

To overcome the above limitations of the PS-MPPT, a random sampling-rate MPPT method for CHB PV inverters is proposed in this paper, which has better interharmonic suppression performances in practice, especially when the number of CHB cells is high. In Section II, the control structure of the CHB PV inverter is briefly introduced, and the interharmonic suppression performance of the PS-MPPT method under varying environmental conditions is analyzed. In Section III, the proposed random sampling-rate MPPT is developed. Subsequently, the proposed method is verified and compared with the PS-MPPT by simulations, and validated by experiments in Section IV. In Section V, concluding remarks are provided.

II. Proposed Random Sampling-rate MPPT Method

A. Control Structure of CHB PV inverters

The control diagram of an n-cell CHB PV inverter is shown in Fig. 3, where a two-layer control consisting of the primary control and the secondary control, is adopted [10], [14]. As shown in Fig. 3, the primary control is responsible for global MPPT tracking of the entire CHB PV system. It sums up all the outputs of individual MPPT controllers as the equivalent total DC voltage reference. Then, through the voltage-outer-loop and current-inner-loop control, the modulation index M_{total} can be calculated and equally distributed to each CHB cell. The

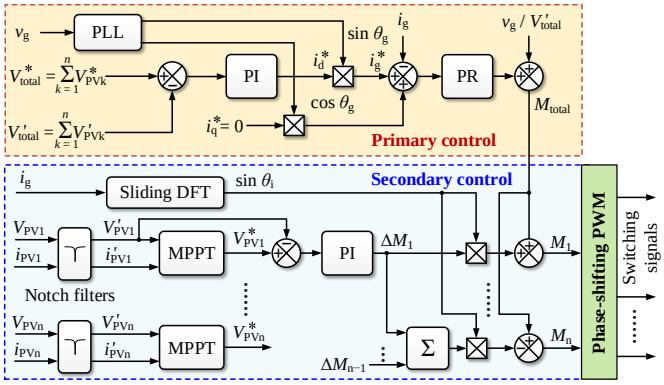

Fig. 3. Control diagram of a single-phase CHB PV inverter (DFT - discrete Fourier transform; PWM - pulse width modulation; PI - proportional integral; PR - proportional resonant), where V'_{PVk} is the filtered DC voltage for the k^{th} cell, V'_{total} is filtered equivalent total DC voltage, and θ_g and θ_i are the phase angles for the grid voltage and current, respectively. i^*_g is the grid current reference, and i^*_d and i^*_q are the current references of the d-axis and q-axis, respectively. M_k indicates the modulation index of the k^{th} H-bridge cell and M_{total} is the equivalent total modulation index.

secondary control is in charge of the individual MPPT by controlling the DC voltage of each cell through a proportional-integral (PI) regulator. With this secondary control, a modified term ΔM_k can be calculated for each cell (k denotes for the index of CHB cells), and added to the equally distributed modulation index M_{total}. As shown in Fig. 3, except for the n^{th} cell, the modulation index for all other cells can be calculated as

$$M_k = M_{total} + \Delta M_k \sin\theta_i \tag{1}$$

where θ_i denotes for the phase angle of the grid current i_g, and it is extracted by a sliding discrete Fourier transform (SDFT) algorithm [14], [15]. For the n^{th} cell, the modulation index should be expressed as

$$M_n = M_{total} - \left(\sum_{k=1}^{n-1} \Delta M_k\right) \sin\theta_i \tag{2}$$

with the above-mentioned two-layer control method, the module-level MPPT can be achieved for the CHB PV inverter.

B. Limitations of the PS-MPPT

In general, the operating point of the PV panel swings around its maximum power point (MPP) as a three-stair voltage waveform in steady state. In this case, each DC voltage will oscillate at one fourth of the MPPT frequency f_{MPPT} [6]. If this oscillation of each CHB cell is in-phase with each other, the oscillation on the equivalent total DC voltage will be n-time higher, as shown in Fig. 2. This magnified voltage oscillation will appear on the amplitude of the current reference, and consequently, higher interharmonics will be generated on the grid current through the control loops. This issue can be solved by the PS-MPPT method in [12], as shown in Fig. 4(a), where the DC voltage oscillations are properly phase-shifted to mitigate the oscillation on the equivalent total DC voltage, and thereby interharmonics. However, for CHB PV inverters with an odd number of cells, the interharmonic suppression per-

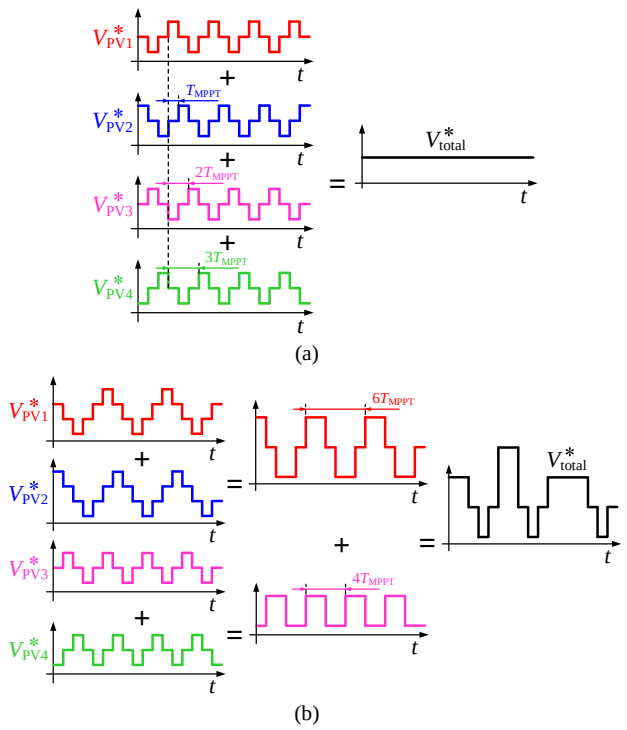

Fig. 4. PV voltage oscillation of the PS-MPPT on a 4-cell CHB PV inverter, where T_{MPPT} indicates the MPPT sampling period: (a) DC voltage references in steady state, and (b) DC voltage references when PV #1 and #2 are under varying environmental conditions.

formance of the PS-MPPT is limited [12], as aforementioned. Moreover, under varying environmental conditions, such as the changes of irradiance and temperature, the DC voltage oscillations may not be optimally phase-shifted. As examplified in Fig. 4(b), if the environmental conditions of PV #1 and #2 change, their DC voltage references will no longer be kept as three-stair waveforms. In this case, since V^*_{PV3} and V^*_{PV4} are still phase-shifted, $(V^*_{PV3}+V^*_{PV4})$ will oscillate at $f_{MPPT}/4$. This oscillation will appear in the equivalent total DC voltage, which induces interharmonics. Thus, under dynamic conditions, interharmonic suppression performance of the PS-MPPT is limited, especially when a high number of cells are cascaded. In that case, it can be challenging to ensure that all the cells are properly phase-shifted to mitigate interharmonics. Therefore, more efforts should be made to overcome the limitations of the PS-MPPT.

C. Proposed Approach

In [7], a modified MPPT method has been proposed for two-level PV inverters to mitigate the interharmonics in the grid current, where f_{MPPT} was randomly selected between two values f_{min} and f_{max} for every MPPT cycle (f_{min} and f_{max} refer to the lower and upper limit of the MPPT frequency). Inspired by this, the random sampling-rates of individual MPPT controllers are applied to the CHB PV inverter in this paper, as illustrated in Fig. 5. As it can be observed in Fig. 5, the MPPT period T_{MPPT} is randomly generated for each cell, and the MPPT algorithm is executed every time when the time counter is reset from the period value to zero. By doing so, the oscillation on the equivalent total DC voltage will become more arbitrary. The

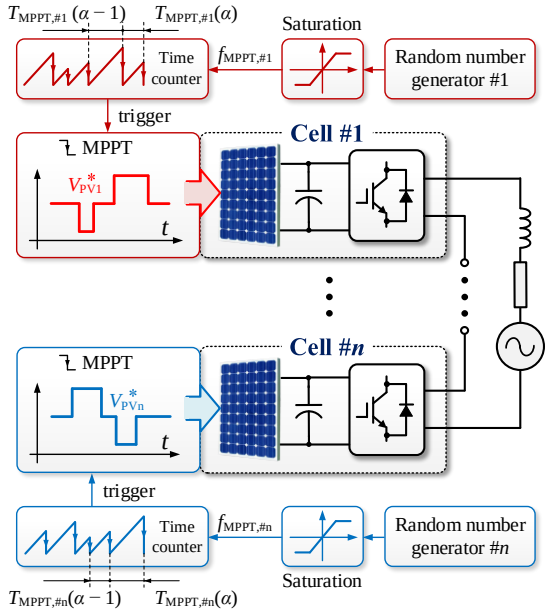

Fig. 5. Control diagram of the random sampling-rate MPPT for CHB PV systems, where $f_{MPPT,\#k}$ refers to the MPPT frequency of the cell #k, and $T_{MPPT,\#k}(\alpha)$ refers to the α^{th} MPPT period of the cell #k.

TABLE I. PARAMETERS OF THE CHB PV INVERTER

PV rated power for each CHB cell	1066 W
DC link capacitor	680 μF
Grid-side L-filter	5.4 mH
Switching frequency of one cell	5 kHz
Controller sampling frequency	10 kHz
Grid voltage (RMS)	220 V
Grid frequency	50 Hz
MPPT sampling rate*	6.7 Hz
MPPT step-size v_{step}	6 V

*refers to the MPPT sampling rate for the conventional MPPT and PS-MPPT

low frequency components will be reduced, and through the control loops, interharmonics will be scattered on a wider range of frequencies, leading to the reduction of the dominant interharmonics. Compared to the PS-MPPT, the random sampling-rate MPPT features a more simple structure for implementation, which can be more feasible for CHB PV inverters with a high number of cells in practice.

III. SIMULATION AND EXPERIMENTAL RESULTS

A. Simulation Results

To validate the effectiveness of the random sampling-rate MPPT method, simulations of the proposed method on a 3-cell and a 4-cell CHB PV inverter have been conducted and compared with the PS-MPPT on MATLAB/Simulink. The simulation results are shown in Figs. 6-8, and the parameters are shown in Table I.

Case 1: Firstly, the performance of the conventional MPPT method on a 3-cell CHB PV inverter is demonstrated in Fig. 6 with a constant irradiance of 100 W/m^2. As it can be observed

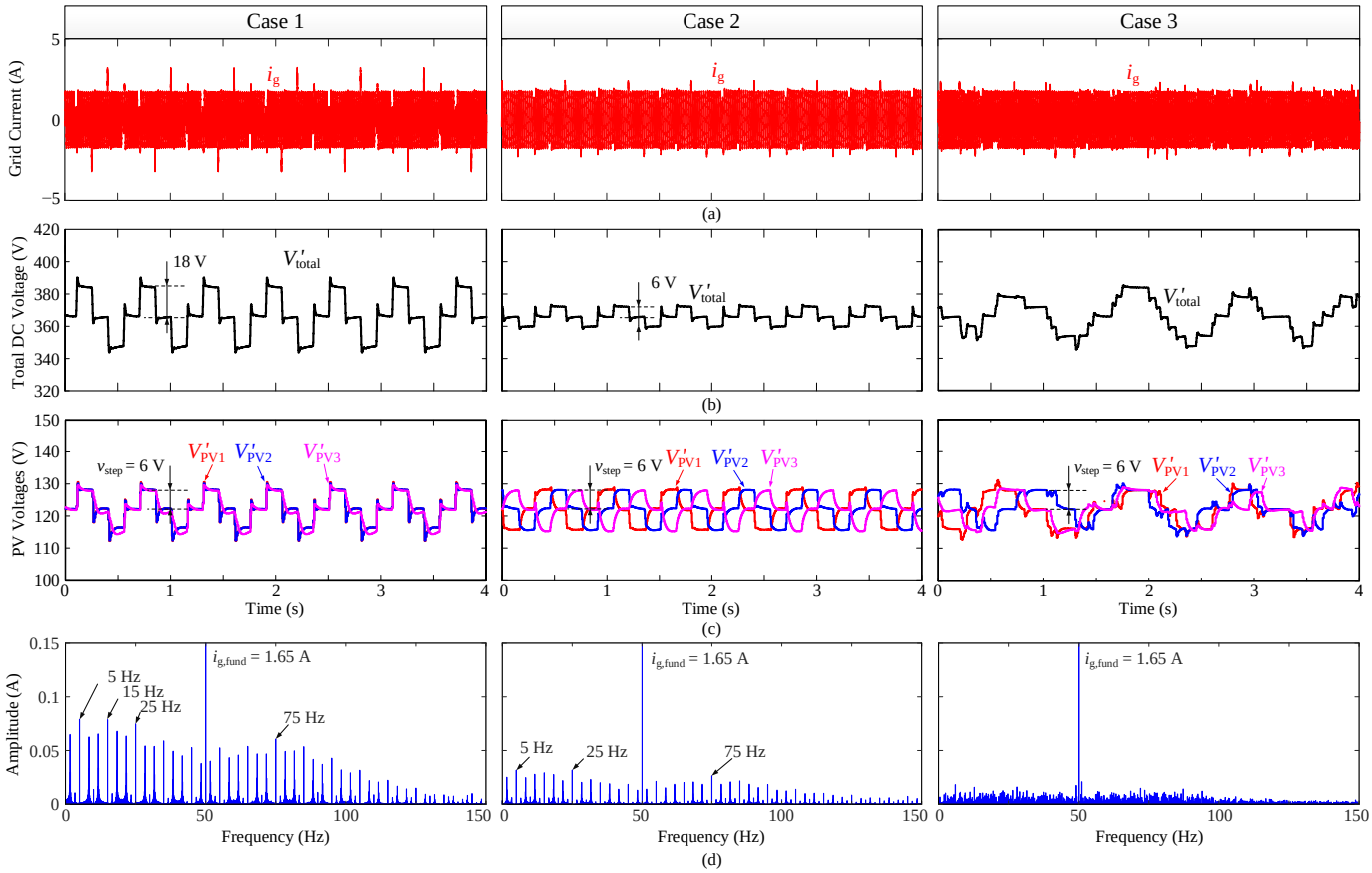

Fig. 6. Simulation results of a 3-cell CHB PV inverter, where $i_{g,fund}$ is the fundamental component of i_g: (a) grid current, (b) the equivalent total DC voltage, (c) DC voltages of 3 CHB cells, and (d) frequency spectrum of the grid current.

in Fig. 6, the perturbations on the DC voltages of all CHB cells are in-phase, leading to an even larger oscillation in the equivalent total DC voltage. The amplitude of the oscillation reaches 18 V (36 V for the peak-to-peak voltage), which is three times higher than the oscillations on one CHB cell. As a result, the grid current has a higher amplitude of oscillations, and large interharmonics can be expected in the grid current, as shown in Fig. 6(d). The dominant interharmonics locate at $50 \pm (2m + 1) \cdot (f_{MPPT} / 4)$ Hz [6], where m = 0, 1, 2…, with the highest amplitude being 0.08 A at 5 Hz.

Case 2: The performance of the PS-MPPT is also shown in Fig. 6, with the same test conditions of Case 1. As shown in Fig. 6, the DC voltage oscillations of cell #2 and #3 are shifted by T_{MPPT} corresponding to cell #1, and consequently, the oscillation amplitude on the equivalent total DC voltage is reduced to 6 V. This is equal to the oscillation on one converter cell. The interharmonics have thus been suppressed, as shown in Fig. 6(d), with the largest interharmonic being 0.03 A at 5 Hz. However, since the periodical oscillation still exists on the total DC voltage, for the 3-cell CHB PV inverter, the PS-MPPT method is only capable to suppress the interharmonics by approximately one third compared to Case 1.

Case 3: To demonstrate the effectiveness of the proposed random sampling-rate MPPT method, simulation results are shown in Fig. 6 with the same test conditions of Case 1. The sampling rate of each CHB cell is randomly selected within the frequency range of 2 Hz to 10 Hz. As shown in Fig. 6, in this case, the oscillation frequency for each CHB cell becomes arbitrary, and consequently, the oscillation on the equivalent total DC voltage randomly varies with its peak-to-peak voltage being about 36 V. The periodic oscillation on the grid current disappears, and the dominant interharmonics are almost eliminated, as shown in the frequency spectrum in Fig. 6(d), where the amplitude of the highest content is around 0.02 A. Due to the random selection of the MPPT rate, the interharmonics are spreading in a wider frequency region, rather than concentrating on particular frequencies. Therefore, compared to the PS-MPPT, the interharmonics can be further suppressed with the proposed random sampling-rate MPPT method for the 3-cell CHB PV inverter.

Case 4: The interharmonic suppression performance of the PS-MPPT under varying environmental conditions is shown in Fig. 7, where a 4-cell CHB PV inverter is tested. The irradiance for PV #1 ramps from 100 W/m^2 to 150 W/m^2 from 6 s to 10 s, and irradiance for PV #2 ramps from 100 W/m^2 to 150 W/m^2 from 8 s to 12 s. As shown in Fig. 7, before t = 6 s, the DC voltage oscillations of all cells are shifted by T_{MPPT}, $2T_{MPPT}$ and $3T_{MPPT}$ for PV #2, #3, and #4 with respect to PV #1, respectively. As a result, the oscillation on the equivalent total DC voltage is almost fully eliminated, as well as the inter-harmonics, as shown in the frequency spectrum in Fig. 7(d).

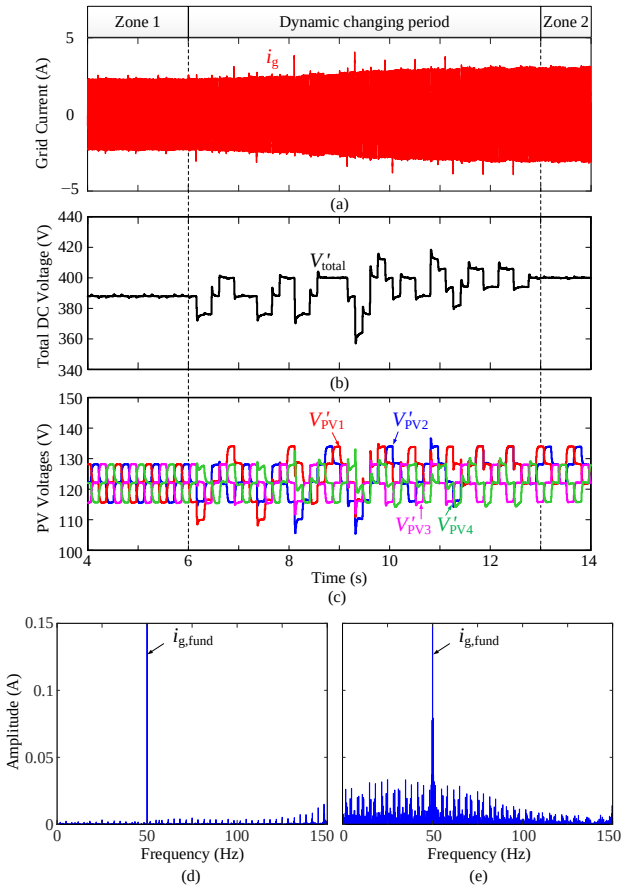

Fig. 7. Simulation results of a 4-cell CHB PV inverter with the PS-MPPT when the irradiance changes: (a) grid current, (b) the equivalent total DC voltage, (c) DC voltages of 4 CHB cells, (d) frequency spectrum of the grid current in zone 1 (before t = 6 s), and (e) frequency spectrum of the grid current in dynamic changing period (between t = 6 s to 13 s).

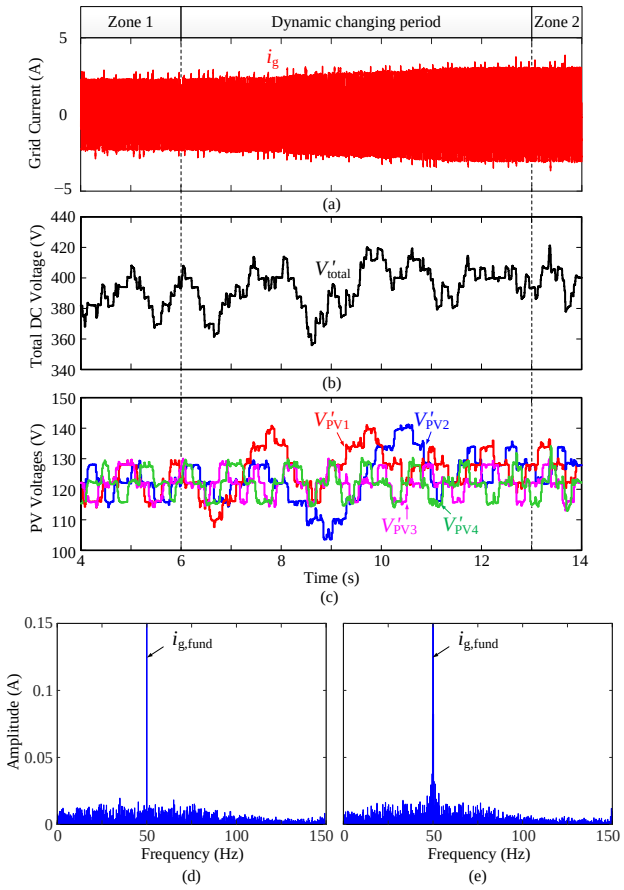

Fig. 8. Simulation results of a 4-cell CHB PV inverter with the proposed random sampling-rate MPPT when the irradiance changes: (a) grid current, (b) the equivalent total DC voltage, (c) DC voltages of 4 CHB cells, (d) frequency spectrum of the grid current in zone 1 (before t = 6 s), and (e) frequency spectrum of the grid current in dynamic changing period (between t = 6 s to 13 s).

However, during t = 6 s to 13 s, due to the slow change of irradiance, the DC voltages of PV #1 and #2 are no longer properly phase-shifted, and interharmonics appear during this period, with the dominant interharmonics being around 0.03 A, as shown in Fig. 7(e).

Case 5: The interharmonic suppression performance of the random sampling rate MPPT under varying environmental conditions is shown in Fig. 8, with the same test conditions for Case 4. As shown in Fig. 8, before t = 6 s, the interharmonics are higher than Case 4. This is because the PS-MPPT can eliminate the oscillation on the total DC voltage for CHB PV inverters with an even number of cells. However, between 6 s to 13 s, the slow change of irradiance does not lead to the increase of interharmonics. As shown in Fig. 8(e), during this period, most interharmonics are below 0.02 A, which indicates that the random sampling-rate MPPT has a better interharmonic performance than the PS-MPPT under varying environmental conditions.

B. Experimental Results

The random sampling-rate MPPT method is further validated on a downscaled 2-cell grid-connected CHB PV inverter, as shown in Fig. 9. The experimental parameters are the same as those listed in Table I, except that 1) the rated PV power for each cell is 300 W, 2) a 40-V(rms) grid is connected due to the limited output voltage of the PV simulator, and 3) the MPPT step-size v_{step} is reduced to 4 V.

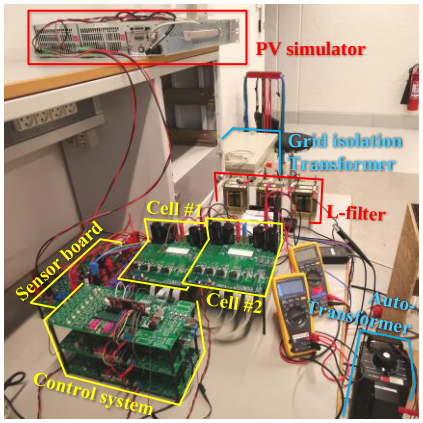

Fig. 9. Photo of the experimental setup of the two-cell CHB PV inverter.

Firstly, the in-phase oscillation phenomenon under the conventional MPPT method is illustrated in Fig. 10(a). As shown in Fig. 10(a), with the in-phase DC voltage oscillations of PV #1 and #2, periodical spikes also appear in the grid

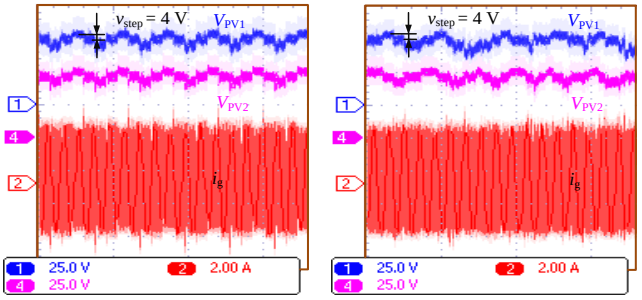

Fig. 10. Experimental results on a 2-cell CHB PV inverter under 200 W/m^2 and 25 °C with the PV rated power being 300 W for each cell, and the grid voltage is 40 V(rms) (V_{PV1} [25 V/div] and V_{PV2} [25 V/div]: DC voltages for cell #1 and #2; i_g [2 A/div]: grid current): (a) with in-phase MPPT perturbations and (b) with the proposed random sampling-rate MPPT control.

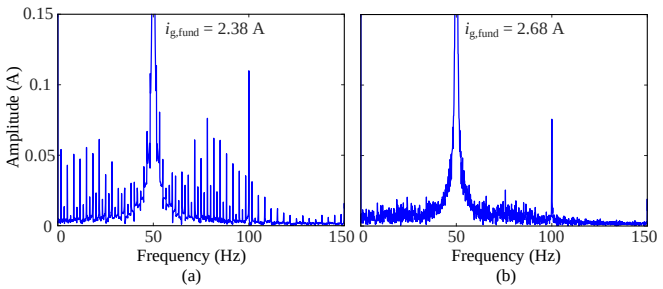

Fig. 11. Fast Fourier transform (FFT) analysis of the grid current i_g shown in Fig. 10: (a) with in-phase MPPT perturbations and (b) with the proposed random sampling-rate MPPT control.

current. This results in the interharmonics of the output current, which can be observed from the frequency spectrum in Fig. 11(a). The dominant interharmonics are around 0.05 A. On the other hand, the experimental results of the proposed random sampling-rate MPPT is demonstrated in Fig. 10(b). In this test, the MPPT sampling-rates of both PV cells randomly vary between 4 Hz to 20 Hz. As shown in the frequency spectrum in Fig. 11(b), compared with Fig. 11(a), it is clear that the interharmonics are effectively suppressed with the proposed random sampling-rate MPPT.

IV. Conclusions

In the CHB PV systems, due to the in-phase oscillation of the DC voltages of CHB cells, the interharmonics in the grid current may be amplified. To address this issue, the PS-MPPT can be employed. However, the PS-MPPT has two limitations: 1) when an odd number of cells are cascaded, the interharmonic suppression performance is degraded; and 2) the interharmonic suppression performance may be affected, especially when a high number of cells are cascaded. To overcome these limitations, a random sampling-rate MPPT method was proposed in this paper for the CHB PV inverters, where the MPPT frequencies were random for individual CHB cells. In this way, the oscillation on the equivalent total DC voltage become arbitrary, and the interharmonics in the grid current were reduced both in steady-state and dynamic conditions. Compared with the PS-MPPT, the random sampling-rate MPPT is simpler and more practical for implementation. Simulations and experimental results have validated the effectiveness of the proposed method.

References

[1] R. Langella, A. Testa, J. Meyer, F. Mller, R. Stiegler, and S. Z. Djokic, "Experimental-based evaluation of PV inverter harmonic and interharmonic distortion due to different operating conditions," *IEEE Trans. Instrum. Meas.*, vol. 65, no. 10, pp. 2221–2233, Oct. 2016.

[2] V. Ravindran, S. K. Rönnberg, and M. H. J. Bollen, "Interharmonics in PV systems: a review of analysis and estimation methods; considerations for selection of an apt method," *IET Renew. Power Gener.*, vol. 13, no. 12, pp. 2023–2032, Sept. 2019.

[3] V. Ravindran, T. Busatto, S. K. Ronnberg, J. Meyer, and M. Bollen, "Time-varying interharmonics in different types of grid-tied PV inverter systems," *IEEE Trans. Power Del.*, vol. 35, no. 2, pp. 483-496, Apr. 2020.

[4] *IEEE Standard for Interconnection and Interoperability of Distributed Energy Resources with Associated Electric Power Systems Interfaces*, IEEE Standard 1547-2018, Apr. 2018.

[5] C. Hou, M. Zhu, Z. Li, Y. Li and X. Cai, "Inter-harmonic THD amplification of voltage source converter: concept and case study," *IEEE Trans. Power Electron.*, DOI: 10.1109/TPEL.2020.2994751.

[6] A. Sangwongwanich, Y. Yang, D. Sera, H. Soltani, and F. Blaabjerg, "Analysis and modeling of interharmonics from grid-connected photovoltaic systems," *IEEE Trans. Power Electron.*, vol. 33, no. 10, pp. 8353-8364, Oct. 2018.

[7] A. Sangwongwanich, and F. Blaabjerg, "Mitigation of interharmonics in PV systems with maximum power point tracking modification," *IEEE Trans. Power Electron.*, vol. 34, no. 9, pp. 8279-8282, Sept. 2019.

[8] A. Sangwongwanich, Y. Yang, D. Sera, and F. Blaabjerg, "Inter-harmonics from grid-connected PV systems: mechanism and mitigation," in *Proc. IFEEC-ECCE Asia*, Jun. 2017, pp. 722–727.

[9] B. Xiao, L. Hang, J. Mei, C. Riley, L. M. Tolbert, and B. Ozpineci, "Modular cascaded H-bridge multilevel PV inverter with distributed MPPT for grid-connected applications," *IEEE Trans. Ind. Appl.*, vol. 51, no. 2, pp. 1722-1731, Mar./Apr. 2015.

[10] Y. Pan, C. Zhang, S. Yuan, A. Chen and J. He, "A decentralized control method for series connected PV battery hybrid microgrid," in *Proc. ITEC Asia-Pacific*, Aug. 2017, pp. 1–6.

[11] H. D. Tafti, A. I. Maswood, G. Konstantinou, C. D. Townsend, P. Acuna, and J. Pou, "Flexible control of photovoltaic grid-connected cascaded H-bridge converters during unbalanced voltage sags," *IEEE Trans. Ind. Electron.*, vol. 65, no. 8, pp. 6229–6238, Aug. 2018.

[12] Y. Pan, A. Sangwongwanich, Y. Yang and F. Blaabjerg, "A phase-shifting MPPT to mitigate interharmonics from cascaded H-bridge PV inverters," *IEEE Trans. Ind. Appl.*, DOI: 10.1109/TIA.2020.3000969.

[13] S. Kouro, P. Lezana, M. Angulo and J. Rodriguez, "Multicarrier PWM with DC-link ripple feedforward compensation for multilevel inverters," *IEEE Trans. Power Electron.*, vol. 23, no. 1, pp. 52-59, Jan. 2008.

[14] J. He, Y. Li, C. Wang, Y. Pan, C. Zhang, and X. Xing, "Hybrid microgrid with parallel- and series-connected microconverters," *IEEE Trans. Power Electron.*, vol. 33, no. 6, pp. 4817-4831, Jun. 2018.

[15] E. Jacobsen and R. Lyons, "The sliding DFT," *IEEE Signal Process. Mag.*, vol. 20, no. 2, pp. 74–80, Mar. 2003.